Infrared Physics & Technology 81 (2017) 1–6

Contents lists available at ScienceDirect

Infrared Physics & Technology

journal homepage: www.elsevier.com/locate/infrared

A method to measure internal stray radiation of cryogenic infrared imaging systems under various ambient temperatures

Qijie Tian [a,b,*], Songtao Chang [a], Zhou Li [a,b], Fengyun He [a], Yanfeng Qiao [a]

[a] *Changchun Institute of Optics, Fine Mechanics and Physics, Chinese Academy of Sciences, Changchun, Jilin 130033, China*
[b] *University of Chinese Academy of Sciences, Beijing 100049, China*

HIGHLIGHTS

- The calibration formula is deduced considering the integration time.
- The effect of ambient temperature on internal stray radiation is analyzed in detail.
- A method is proposed to measure internal stray radiation of cryogenic infrared imaging systems.
- Experimental results indicate that the proposed method can measure internal stray radiation accurately.

ARTICLE INFO

Article history:
Received 13 October 2016
Revised 5 December 2016
Accepted 6 December 2016
Available online 9 December 2016

Keywords:
Internal stray radiation
Cryogenic infrared imaging system
Ambient temperature
Radiometric calibration

ABSTRACT

The suppression level of internal stray radiation is a key criterion for infrared imaging systems, especially for high-precision cryogenic infrared imaging systems. To achieve accurate measurement for internal stray radiation of cryogenic infrared imaging systems under various ambient temperatures, a measurement method, which is based on radiometric calibration, is presented in this paper. First of all, the calibration formula is deduced considering the integration time, and the effect of ambient temperature on internal stray radiation is further analyzed in detail. Then, an approach is proposed to measure the internal stray radiation of cryogenic infrared imaging systems under various ambient temperatures. By calibrating the system under two ambient temperatures, the quantitative relation between the internal stray radiation and the ambient temperature can be acquired, and then the internal stray radiation of the cryogenic infrared imaging system under various ambient temperatures can be calculated. Finally, several experiments are performed in a chamber with controllable inside temperatures to evaluate the effectiveness of the proposed method. Experimental results indicate that the proposed method can be used to measure internal stray radiation with high accuracy at various ambient temperatures and integration times. The proposed method has some advantages, such as simple implementation and the capability of high-precision measurement. The measurement results can be used to guide the stray radiation suppression and to test whether the internal stray radiation suppression performance meets the requirement or not.

1. Introduction

Stray radiation, known as stray light, refers to the unwanted radiation or light that reaches the image plane. Stray radiation can reduce the signal to noise ratio (SNR) of images and influence the detectivity of systems. Efficient control of stray radiation is required for all imaging systems [1–4]. Stray radiation can be divided into two categories: external stray radiation and internal stray radiation. The external stray radiation arises from the radiation that is emitted by the thermal sources outside the field of view (FOV) and reaches the image plane through some optical paths, such as reflection, scatter or transmission [5,6]. The internal stray radiation mainly originates from the thermal radiation of structures scattered by surfaces and the self-radiation of lens [7,8]. For infrared imaging systems, apart from the external stray radiation, internal stray radiation will have an effect on the system as well. In order to detect small temperature differences, typical infrared imaging systems with high precision employ the cryogenic infrared detectors, which are extraordinarily sensitive to thermal sources. Internal stray radiation will have a significant effect on

* Corresponding author at: Changchun Institute of Optics, Fine Mechanics and Physics, Chinese Academy of Sciences, Changchun, Jilin 130033, China.
E-mail address: tian7jie@163.com (Q. Tian).

http://dx.doi.org/10.1016/j.infrared.2016.12.004
1350-4495/

cryogenic infrared systems. Consequently, accurate measurement of internal stray radiation is of great significance, such as to evaluate the internal stray radiation suppression level, or to guide the design of stray radiation suppression. Current papers and patents are mainly focused on the stray radiation analysis and suppression, as well as the test of external stray radiation suppression performance. Few investigations however have been conducted with respect to the measurement of internal stray radiation of cryogenic infrared imaging systems.

Generally, the test of stray radiation suppression performance can be briefly classified into two categories. (1) By building the analytical model, the stray radiation can be analyzed quantitatively using the Monte Carlo method, ray tracing method, parallel calculation method, etc. Typical analysis programs are TracePro, Lighttools, Zemax, ASAP, FRED, etc. [8–10]. The simulation method has the advantages of simple implementation, no demand for experimental conditions, lower cost and so on. Whereas, its drawbacks lie in the fact that it may produce significant errors due to the deviation from the bidirectional reflectance distribution function (BRDF) of actual surfaces and the characteristics of lens. (2) The stray radiation needs to be measured after the infrared imaging system has been fabricated. According to the measurement results, the system may need to be modified slightly to improve the stray radiation suppression performance [10–12]. Nevertheless, the measurement results include external stray radiation and internal stray radiation for infrared imaging systems, which means we are unable to directly acquire the internal stray radiation. Besides, current measurement methods need to be performed under various ambient temperatures using expensive equipments, which have the problems of high cost, long duration and complicated operation.

By analyzing the factors that result in internal stray radiation, this article introduces a method to measure the internal stray radiation of cryogenic infrared imaging systems under various ambient temperatures. A short outline of this paper is as follows: in Section 2, the radiometric calibration formula is deduced considering the integration time, and the effect of ambient temperature on internal stray radiation is further discussed in detail. In Section 3, the details of the proposed approach are given. In Section 4, experiments are conducted in a chamber with controllable inside temperatures to verify the measurement accuracy of the proposed approach. The conclusion is given in Section 5.

2. Effect of ambient temperature on radiometric calibration

As all substances above absolute zero unceasingly emit radiation which is proportional to their temperatures, the internal stray radiation of an infrared imaging system is in connection with the ambient temperature, which will have an effect on the radiometric calibration [13,14]. Besides, the output gray value caused by internal stray radiation will change along with the integration time variation, which should be analyzed. In this section, we first introduce the calibration formula considering the integration time. Then, the effect of ambient temperature on internal stray radiation is further discussed in detail. Finally, a calibration formula is deduced at arbitrary integration times and ambient temperatures.

2.1. Radiometric calibration considering the integration time

In this paper, the near-extended-source method is adopted to perform radiometric calibration at a selected integration time. The relation between the output gray value (digital number, DN) and the incident radiance is linear within the linear response range of a cooled mid-wave infrared (MWIR) detector, and can be expressed as [15]

$$h_{i,j} = G_{i,j} \cdot L_t + B_{i,j}, \tag{1}$$

where $h_{i,j}$ denotes the output gray value of the (i,j)th detector pixel in the focal plane array (FPA), $G_{i,j}$ is the response to the incident radiance of the blackbody, and $B_{i,j}$ denotes the offset. The incident radiance can be obtained by [16]

$$L_t = \varepsilon \cdot L(T_t) = \frac{\varepsilon}{\pi} \int_{\lambda_1}^{\lambda_2} M(\lambda, T_t) d\lambda, \tag{2}$$

where $L(T_t)$ is the in-band radiance of an ideal blackbody at the absolute temperature T_t, ε denotes the emissivity of the reference source, $\lambda_1 \sim \lambda_2$ is the integration spectral range, and $M(\lambda, T_t)$ is the spectral radiant exitance calculated by Plank's formula. The schematic of near-extended-source method is exhibited in Fig. 1.

The incident radiation flux that reaches a detector pixel can be calculated by [17,18]

$$\Phi_t = \frac{\pi \cdot \varepsilon \cdot \tau}{4} \cdot \left(\frac{D}{f}\right)^2 \cdot A_d \cdot L(T_t) = K_t \cdot L(T_t), \tag{3}$$

where D is the diameter of optics, f denotes the focal length of optics, τ is the transmissivity of optics, and A_d is the sensitive area of a detector pixel. Thereupon, K_t is constant for a given infrared imaging system. The response of a detector pixel to the incident radiance flux can be written as $G'_{i,j} = G_{i,j}/K_t$.

The offset $B_{i,j}$ is caused by the internal stray radiation of infrared imaging systems and the internal factors of cryogenic infrared detector, such as the dark current. Consequently, $B_{i,j}$ can be expressed as

$$B_{i,j} = G'_{i,j} \cdot \Phi_{stray,i,j} + h_{det,i,j}, \tag{4}$$

where $\Phi_{stray,i,j}$ is the flux resulting from internal stray radiation, and $h_{det,i,j}$ denotes the output gray value originating from internal factors of the detector.

When the infrared imaging system is calibrated at a selected integration time, the response $G'_{i,j}$ is obviously proportional to the integration time, and can be given by $G'_{i,j} = t \cdot G'_{0,i,j}$, where t is the integration time and $G'_{0,i,j}$ is the response of the (i,j)th detector pixel at unit integration time [19]. Moreover, experiments have illustrated that $h_{det,i,j}$ has a linear relation to the integration time as well, and the relation can be expressed as [20]

$$h_{det,i,j}(t) = t \cdot h_{det1,i,j} + h_{det2,i,j}, \tag{5}$$

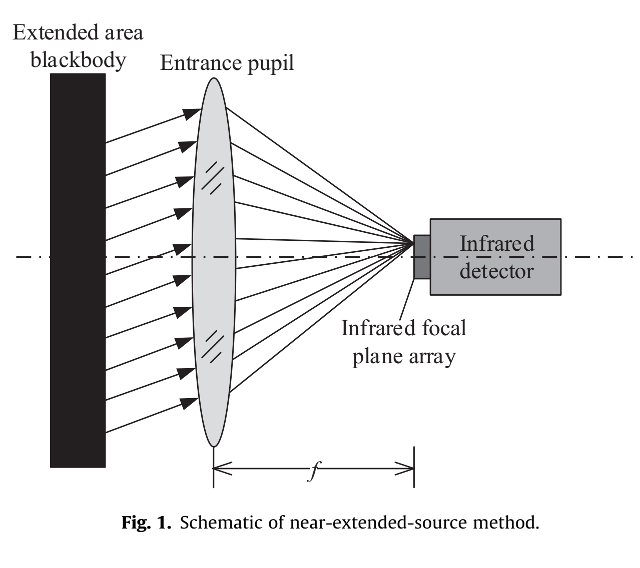

Fig. 1. Schematic of near-extended-source method.

where $h_{det1,i,j}$ refers to the factors that have a linear relation to the integration time and $h_{det2,i,j}$ refers to the factors that are independent of the integration time.

Neglecting the subscription of the detector pixel (i, j) above, the calibration formula considering the integration time can be rewritten as

$$h(t) = t \cdot G'_0 \cdot \Phi_t + t \cdot G'_0 \cdot \Phi_{stray} + t \cdot h_{det1} + h_{det2}. \quad (6)$$

As shown in Eq. (6), the incident radiation flux is determined by the reference source which is independent of the ambient temperature. To be able to detect small temperature variations, the infrared detector is enclosed in a small cryogenic chamber, where the temperature is kept constant (i.e., 77 K). Hence, it is reasonable to make an assumption that the internal factors of the cryogenic infrared detector are independent of the ambient temperature as well. The radiation flux originating from internal stray radiation, however, is apparently in connection with the ambient temperature which will be discussed in detail in next subsection.

2.2. Effect of ambient temperature on internal stray radiation

Experiments have indicated that the output gray value drifts with ambient temperature fluctuation, which is caused by the internal stray radiation. In this subsection, we studied the effect of ambient temperature on internal stray radiation.

Internal stray radiation, for a cryogenic infrared imaging system, is mainly caused by the self-radiation of lens, housing cones and other structures, as well as the narcissus signature [17]. The narcissus signature is a unique stray radiation effect that exists in cryogenic infrared imaging systems, which is caused by the radiation of the cold stop retro-reflected from lens surfaces. In other words, the cryogenic infrared detector "see" its own image. The narcissus signature can be weakened by lowering the reflectivity of critical surfaces [21–23]. Furthermore, the narcissus signature, for a given infrared imaging system with settled lens and structures, is independent of the ambient temperature. Therefore, it is reasonable to subsume the narcissus signature into $h_{det}(t)$.

As we all know, the radiation of lens and other components is determined by their own temperatures. The temperature of the components turns to become uniform namely the ambient temperature, owing to their thermal conductivity. Consequently, it is rational to make an assumption that all components of the infrared imaging system are at the ambient temperature except the cryogenic infrared detector and its surroundings.

In practice, a system can be regarded as an entity that is constituted by proper amount of elements. The internal stray radiation flux can be therefore treat as a summation of contributions from different elements. Suppose an component element dA emitting a small solid angle of stray light bundle, which is finally received by a detector pixel (i, j) through some optical paths. There may be reflection, absorption, transmission, scatter, or any composition among those optical paths [7]. The scattering path of internal stray radiation is sketched in Fig. 2 in detail.

The radiation flux of dA that is received by detector pixel (i, j) can be expressed by

$$d\Phi_{stray}(T_{amb}) = \varepsilon(\theta, \varphi) \cdot dA \cdot \Omega \cdot \tau \cdot \rho \cdot L(T_{amb}), \quad (7)$$

where $\varepsilon(\theta, \varphi)$ denotes the in-band emissivity of element dA in the direction of (θ, φ), Ω is the projected solid angle, the temperature of the element dA equals to the ambient temperature T_{amb}, τ denotes the transmissivity of the bundle from element dA to detector pixel (i, j), ρ refers to the scatter of the bundle from element dA to detector pixel (i, j), and $L(T_{amb})$ is the radiance of an ideal blackbody at the ambient temperature T_{amb}.

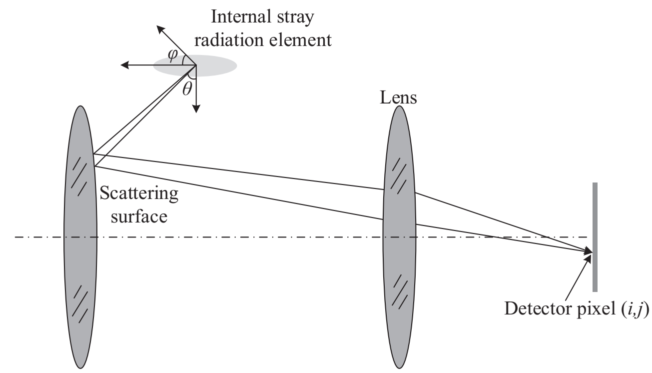

Fig. 2. Schematic of internal stray radiation.

The total radiation flux emitted by lens and structures that is received by detector pixel (i, j) can be calculated by

$$\Phi_{stray}(T_{amb}) = \sum_{i=1}^{M} \varepsilon(\theta_i, \varphi_i) \cdot A_i \cdot \Omega_i \cdot \tau_i \cdot \rho_i \cdot L(T_{amb}), \quad (8)$$

where M is the total number of elements, $\Phi_{stray}(T_{amb})$ is the flux resulting from internal stray radiation at the ambient temperature T_{amb}. As $\sum_{i=1}^{M} \varepsilon(\theta_i, \varphi_i) \cdot A_i \cdot \Omega_i \cdot \tau_i \cdot \rho_i$ is constant for a given infrared system, Eq. (8) can be simplified as

$$\Phi_{stray}(T_{amb}) = K_{stray} \cdot L(T_{amb}), \quad (9)$$

where $K_{stray} = \sum_{i=1}^{M} \varepsilon(\theta_i, \varphi_i) \cdot A_i \cdot \Omega_i \cdot \tau_i \cdot \rho_i$. It is illustrated in Eq. (9) that the flux originating from internal stray radiation of an infrared imaging system is in direct proportion to the radiance of an ideal blackbody at the ambient temperature.

By submitting Eqs. (9)–(6), we can yield the calibration formula at arbitrary integration times and ambient temperatures, which can be expressed as

$$h(t, T_{amb}) = t \cdot G_0 \cdot L_t + t \cdot G_{stray} \cdot L(T_{amb}) + t \cdot h_{det1} + h_{det2}, \quad (10)$$

where $G_{stray} = K_{stray} \cdot G'_0$. As shown in Eq. (10), the output gray value originating from internal stray radiation is directly proportional to the integration time and the radiance of an ideal blackbody at the ambient temperature.

3. Method to measure internal stray radiation under various ambient temperatures

According to Eq. (10), the output gray value, caused by internal stray radiation at arbitrary integration times and ambient temperatures, can be calculated as long as the parameter G_{stray} is obtained previously. In order to achieve the measurement of internal stray radiation, we suppose that the infrared imaging system is calibrated at a selected integration time under two ambient temperatures, namely T_{amb1} and T_{amb2}. The calibration formulas are presented as follows

$$h(t_1, T_{amb1}) = t_1 \cdot G_0 \cdot L_t + t_1 \cdot G_{stray} \cdot L(T_{amb1}) + t_1 \cdot h_{det1} + h_{det2}, \quad (11)$$

$$h(t_1, T_{amb2}) = t_1 \cdot G_0 \cdot L_t + t_1 \cdot G_{stray} \cdot L(T_{amb2}) + t_1 \cdot h_{det1} + h_{det2}. \quad (12)$$

The parameter G_{stray}, for the given infrared imaging system, can be calculated by

$$G_{stray} = \frac{h(t_1, T_{amb1}) - h(t_1, T_{amb2})}{t_1 \cdot [L(T_{amb1}) - L(T_{amb2})]}. \quad (13)$$

Thus, the output gray value, caused by internal stray radiation at arbitrary integration times and various ambient temperatures, can be represented as

$$h_{stray}(t, T_{amb}) = t \cdot G_{stray} \cdot L(T_{amb}) = \frac{t}{t_1} \cdot \frac{h(t_1, T_{amb1}) - h(t_1, T_{amb2})}{[L(T_{amb1}) - L(T_{amb2})]} \cdot L(T_{amb}). \quad (14)$$

By submitting Eqs. (13)–(9), the flux originating from internal stray radiation can be expressed as

$$\Phi_{stray}(T_{amb}) = \frac{G_{stray} \cdot K_t}{G_0} \cdot L(T_{amb}), \quad (15)$$

where pertinent parameters have been acquired previously. It is illustrated in Eq. (15) that the flux originating from internal stray radiation is independent of the integration time.

As we can see from Eqs. (14) and (15), the output gray value and flux arising from internal stray radiation under various ambient temperatures can be calculated for a given infrared imaging system, instead of performing the measurement repeatedly. Besides, only two calibration results under two ambient temperatures are required to obtain the internal stray radiation of arbitrary integration times and ambient temperatures, which can naturally reduce the complexity and the time that measurement requires. Compared with typical measurement methods, the proposed approach can directly obtain the internal stray radiation rather than a comprehensive measurement result including both internal and external stray radiation. One of the drawbacks of the proposed method is to control the infrared imaging system at two ambient temperatures, which may be difficult for large aperture infrared systems.

4. Experiments

4.1. Experimental setup

To validate the measurement method proposed above experimentally, the experiments were conducted with a mid-wave infrared imaging system. The aperture of the system is 50 mm, and the focal length is 100 mm. To ensure good performance, the experiments were carried out in a chamber with controllable inside temperatures. Experiments show that the temperature accuracy inside the chamber can be controlled within ±0.5 °C in several minutes as long as the chamber's temperature is set. The SR-800-4A extended-area blackbody, which is selected as the reference source, is manufactured by CI systems; exhibits an effective emissivity of 0.97 in 3.7–4.8 μm waveband and has a 100 mm × 100 mm size. Its temperature accuracy is ±0.01 °C over the operating range from 0 °C to 125 °C. The cryogenic MWIR detector of forward looking infrared (FLIR) systems operates in 3.7–4.8 μm waveband, and has a focal plane array of 640 × 512 pixels with a 14 bit digital output.

The whole system, including the infrared imaging system, the MWIR detector as well as the blackbody, is put inside the chamber. The experimental setup is displayed in Fig. 3.

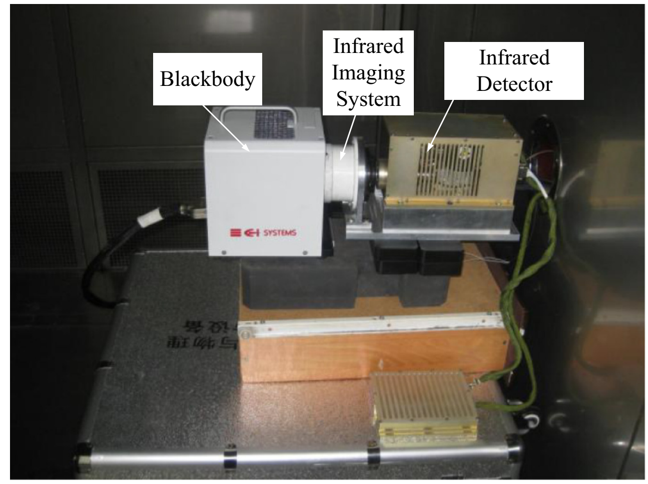

Fig. 3. Experimental setup for radiometric calibration.

4.2. Measurement results and analysis

In order to measure the internal stray radiation of our infrared imaging system, the ambient temperature is set to 30 °C and 20 °C. Each of the ambient temperatures last at least for 40 min to make sure that all parts of the system are at the equal temperature. The temperature of the blackbody is set to 30 °C, 40 °C, 50 °C as well as 60 °C, and the integration time is chosen as 1 ms for simplicity. According to the calibration results and Eq. (13), we obtain $G_{stray} = 245.71 \text{DN} \cdot \text{ms}^{-1} \cdot \text{W}^{-1} \cdot \text{m}^2 \cdot \text{sr}$. Consequently, the output gray value, caused by internal stray radiation at arbitrary integration times and ambient temperatures, can be calculated by

$$h_{stray}(t, T_{amb}) = 245.71 \times t \times L(T_{amb}). \quad (16)$$

For our infrared imaging system, $K_t = 0.4418 \times 10^{-10}\ \text{m}^2 \cdot \text{sr}$. According to the radiometric calibration results, the response of the cryogenic infrared detector, namely G_0, is $2086.29 \text{DN} \cdot \text{ms}^{-1} \cdot \text{W}^{-1} \cdot \text{m}^2 \cdot \text{sr}$. Therefore, the flux originating from internal stray radiation can be calculated by

$$\Phi_{stray}(T_{amb}) = \frac{G_{stray} \cdot K_t}{G_0} \cdot L(T_{amb}) = 5.20 \times 10^{-12} \times L(T_{amb}). \quad (17)$$

According to Eqs. (16) and (17), when the ambient temperature changes, the output gray value and the flux resulting from internal stray radiation can be updated instead of conducting the measurement repeatedly.

To evaluate the performance of the proposed method, the temperature inside the chamber is set to varying from 10 °C to 50 °C with an interval of 5 °C. Similarly, each of the ambient temperatures last at least for 40 min to ensure that all components of the system is at the same temperature. The temperature of the blackbody is still set to 30 °C, 40 °C, 50 °C and 60 °C. Moreover, the measurement method proposed in previous published article [20] is adopted to perform a contrast. The approach proposed in article [20] is denoted as Method One. Both of the measurement results at the integration time of 1 ms are shown in Fig. 4. And the measurement errors are shown in Fig. 5.

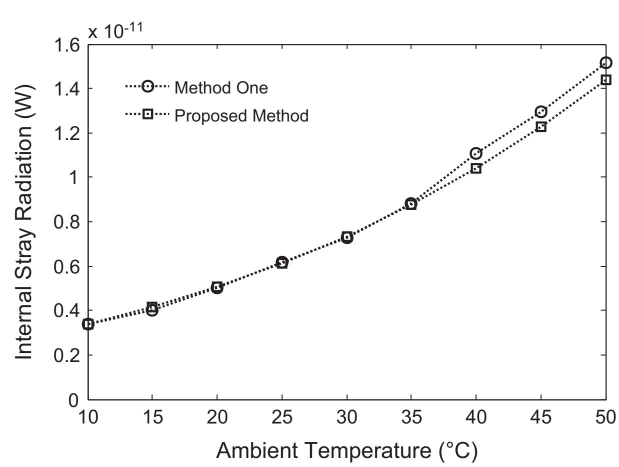

Fig. 4. Measurement results of internal stray radiation at 1 ms.

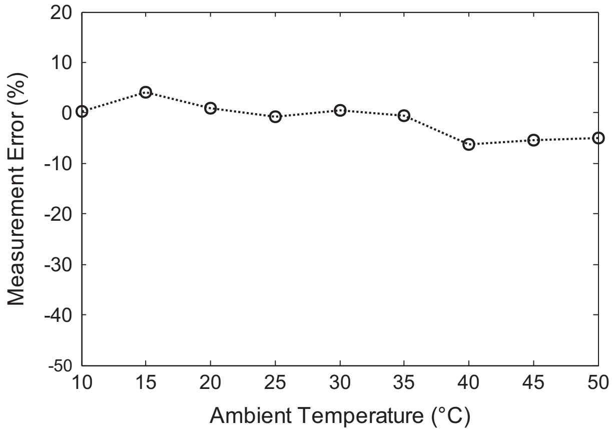

Fig. 5. Measurement errors of internal stray radiation at 1 ms.

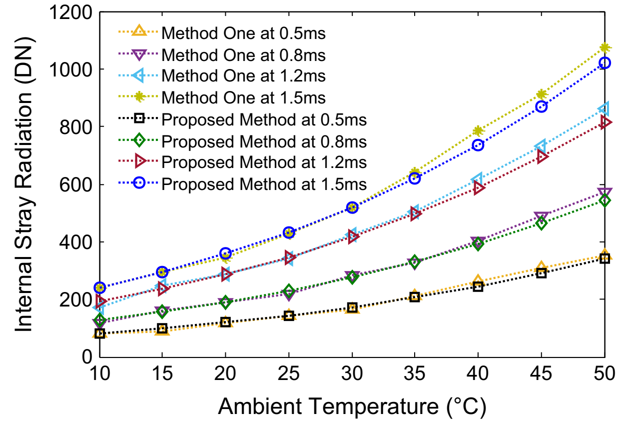

Fig. 7. Output gray value caused by internal stray radiation at several integration times.

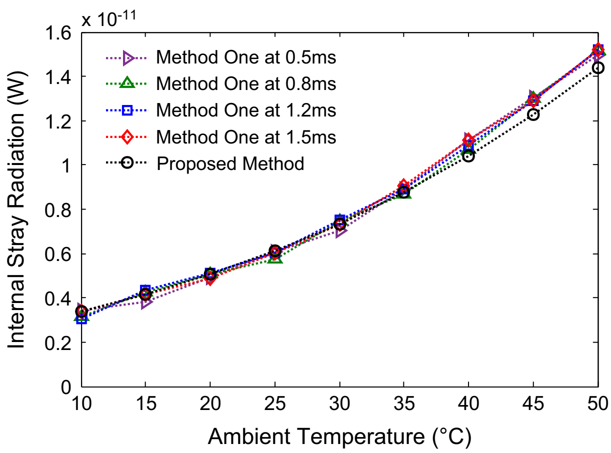

Fig. 6. Flux originating from internal stray radiation at several integration times.

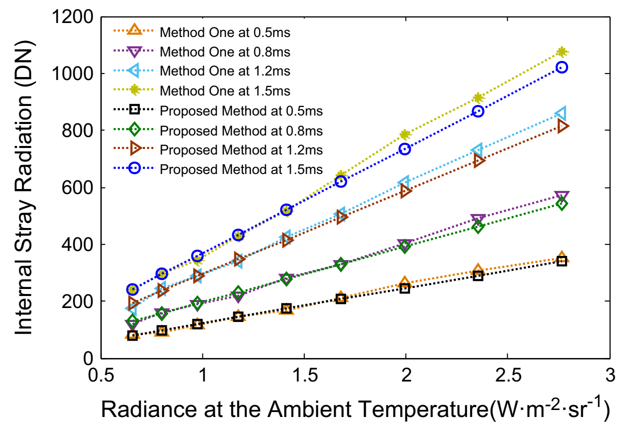

Fig. 8. Internal stray radiation as a function of the radiance at the ambient temperature.

As shown in Fig. 4, the flux originating from internal stray radiation increases rapidly with ambient temperature rising, and the measurement results of the proposed method are coincident well with the results of Method One, which demonstrate that the proposed method is valid for the our infrared imaging system. Fig. 5 shows that the maximum measurement error between the two methods reaches only −6.17%, which is acceptable for infrared imaging systems. Furthermore, there is no tendency for the measurement error to rise or decrease with the ambient temperatures variation, which means the proposed method is stable. The measurement errors are mainly caused by the fluctuation of temperatures inside the chamber. For example, the temperature inside the chamber is set to 20 °C, the actual temperature inside the chamber however may be a little higher or lower than 20 °C. But the temperature fluctuation has a moderate impact on the whole measurement.

To further evaluate the proposed approach, the integration time is set to 0.5 ms, 0.8 ms, 1.2 ms and 1.5 ms, and Method One is adopted to measure the output gray value and the flux resulting from internal stray radiation. As a comparison, the output gray value and the flux, originating from internal stray radiation at various integration times and ambient temperatures, can be directly calculated according to Eqs. (16) and (17), instead of performing the measurement repeatedly. All the measurement results are shown in Figs. 6 and 7, and Fig. 8 shows the output gray values as a function of the radiance at the ambient temperature. The measurement errors are shown in Fig. 9.

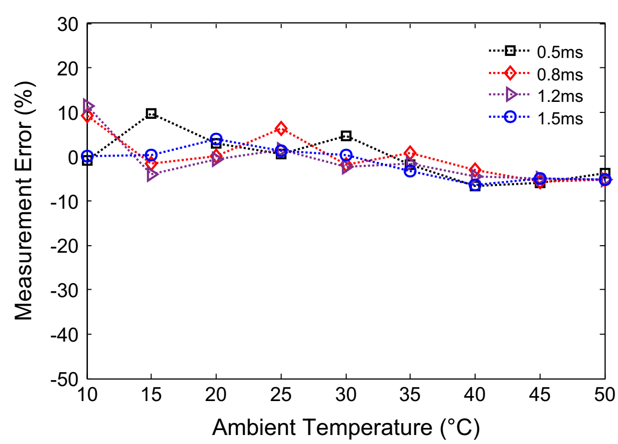

Fig. 9. Measurement errors of internal stray radiation at several integration times.

It is illustrated in Figs. 6 and 7 that the internal stray radiation increases rapidly with the rising of ambient temperature. The flux acquired at different integration times is in good agreement with each other, which demonstrates that the flux resulting from internal stray radiation is independent of the integration time. And the output gray value caused by internal stray radiation is in direct proportion to the integration time, which is in accordance with the theoretical analysis. Besides, the results of the proposed approach are consistent well with the results of Method One at several integration times, which proves that the proposed method can achieve high precious measurement of internal stray radiation under various integration times and ambient temperatures. It is illustrated in Fig. 8 that the output gray values exhibit a linear relation to the radiance at the ambient temperature, which is consistent with the theoretical analysis. And the lines at the same integration time agree well with each other, which further proves that the measurement results of the proposed method are correct. There is still no tendency for the measurement error to rise or decrease with the variation of integration time and ambient temperature. The maximum measurement error is 11.41%, which is mainly caused by the temperature fluctuation inside the chamber as before.

In summary, the approach proposed in this paper can yield high-precision measurement of internal stray radiation at various integration times and ambient temperatures. Moreover, only two calibration results at two ambient temperatures is needed to acquire the internal stray radiation at arbitrary integration times and ambient temperatures. The complexity and time that the measurement requires can be naturally shortened.

5. Conclusions

This paper has introduced a measurement method, which is based on radiometric calibration, to measure the internal stray radiation of cryogenic infrared imaging systems under various ambient temperatures. And the effectiveness of the proposed method has been verified by experiments. By calibrating the cryogenic infrared imaging system under two ambient temperatures, the quantitative relation between the internal stray radiation and the ambient temperature can be obtained, and then the internal stray radiation under various ambient temperatures can be calculated instead of performing the measurement repeatedly. Experiments were conducted in a chamber with controllable inside temperatures. And experimental results show that when the ambient temperature rises from 10 °C to 50 °C, the maximum measurement error is only 11.41%, which demonstrates that the proposed method can achieve high-precision measurement of internal stray radiation at various integration times and ambient temperatures. Moreover, there is no tendency for the measurement error to rise or decrease with the variation of ambient temperature and integration time, which proves that the presented approach is stable. The measurement error is mainly caused by the temperature fluctuation inside the chamber, whose effect on the measurement is moderate.

The proposed method can accurately measure the internal stray radiation under various ambient temperatures by calibrating the system at two ambient temperatures, instead of performing the measurement under every ambient temperature. The complexity and time that the measurement requires is naturally reduced. The proposed method can be used to evaluate whether the suppression performance of internal stray radiation satisfies the system's requirement or not.

References

[1] M.M. Talha, J. Chang, Y. Wang, T. Zhang, D. Cheng, Z. Hui Sun, Design, tolerancing and stray light analyses of a freeform HMD optical system, Optik 121 (2010) 750–755.

[2] M.J. Sholl, F.S. Grochocki, J.C. Fleming, R.W. Besuner, P. Jelinsky, M.L. Lampton, Stray light design and analysis of the SNAP telescope, Proc. SPIE 6675 (2007) 66750C.

[3] S.M. Nejad, A.B. Madineh, M. Nasiri, Baffle design and evaluation of the effect of different parameters on its performance, Optik 124 (2013) 6480–6484.

[4] J.X. Niu, S.H. Shi, R.K. Zhou, Analysis to stray radiation of infrared detecting system, Proc. SPIE 8193 (2011) 81931H.

[5] C.R. Boshuizen, T.R. Bedding, M.L. Pfitzner, M.G. Grimminck, H. Kjeldsen, A.G. Monger, MONS space telescope, part 2: analysis of very high stray-light rejection, Opt. Eng. 47 (1) (2008) 013001.

[6] P.A. Lightsey, Z. Wei, D.L. Skelton, C.W. Bowers, K.I. Mehalick, S.R. Thomson, P. Knollenberg, J.W. Arenberg, Stray light performance for the James Webb Space Telescope, Proc. SPIE 9143 (2014) 91433P.

[7] Y. Liu, X.Q. An, Q. Wang, Accurate and fast stray radiation calculation based on improved backward ray tracing, Appl. Opt. 52 (2013) B1–B9.

[8] Y. Zhu, X. Zhang, T. Liu, Y.X. Wu, G.W. Shi, L.J. Wang, Internal and external stray radiation suppression for LWIR catadioptric telescope using non-sequential ray tracing, Infrared Phys. Technol. 71 (2015) 163–170.

[9] A.V. Pravdivtsev, M.N. Akram, Simulation and assessment of stray light effects in infrared cameras using non-sequential ray tracing, Infrared Phys. Technol. 60 (2013) 306–311.

[10] E. Fest, Stray Light Analysis and Control, 2013.

[11] F. Grochocki, J. Fleming, Stray light testing of the OLI Telescope, Proc. SPIE 7794 (2010) 77940W.

[12] R. Birki, G. Lange, S. Manhart, R. Maurer, Stray radiation measurement on the infrared background signature survey (IBSS) telescope, Proc. SPIE 0967 (1989) 78–89.

[13] R. Siegel, J.R. Howell, Thermal Radiation Heat Transfer, CRC Press, 1992.

[14] Y. Lü, X. He, Z.H. Wei, Z.Y. Sun, S.T. Chang, Ambient temperature-independent dual-band mid-infrared radiation thermometry, Appl. Opt. 55 (2016) 2169–2174.

[15] Z.Y. Sun, S.T. Chang, W. Zhu, Radiometric calibration method for large aperture infrared system with broad dynamic range, Appl. Opt. 54 (2015) 4659–4666.

[16] Y. Té, P. Jeseck, I. Pépin, C. Camy-Peyret, A method to retrieve blackbody temperature errors in the two points radiometric calibration, Infrared Phys. Technol. 52 (2009) 187–192.

[17] S.T. Chang, Y.Y. Zhang, Z.Y. Sun, M. Li, Method to remove the effect of ambient temperature on radiometric calibration, Appl. Opt. 53 (2014) 6274–6279.

[18] B.G. Grant, The Art of Radiometry, 2009.

[19] Y. Jin, J. Jiang, G.J. Zhang, Three-step nonuniformity correction for a highly dynamic intensified charge-coupled device star sensor, Opt. Commun. 285 (2012) 1753–1758.

[20] S.T. Chang, Z.Y. Sun, Y.Y. Zhang, Z. Wei, Internal stray radiation measurement for cooled infrared imaging systems, Acta Phys. Sin. –Chin. Ed. 64 (2015) 887–892.

[21] F.Y. He, J.C. Cui, S.L. Feng, X. Zhang, Narcissus analysis for cooled staring IR system, Proc. SPIE 6722 (2007) 67224N.

[22] M.N. Akram, Simulation and control of narcissus phenomenon using nonsequential ray tracing. I. Staring camera in 3–5 μm waveband, Appl. Opt. 49 (2010) 964–975.

[23] Y. Liu, X.B. Zhong, N. Zhong, C.S. Zheng, L.Z. Wen, Accurate and fast narcissus calculation based on sequential ray trace, Appl. Opt. 52 (2013) 7899–7903.